2550 *Inorg. Chem.* **2010**, *49*, 2550–2556
DOI: 10.1021/ic902463t

Inorganic Chemistry
Article

Syntheses and Characterizations of $Cs_2Cr_3(BP_4O_{14})(P_4O_{13})$ and $CsFe(BP_3O_{11})$ Compounds with Novel Borophosphate Anionic Partial Structures

Weilong Zhang,[†,‡] Wendan Cheng,[*,†] Hao Zhang,[†] Lei Geng,[†,‡] Yeyu Li,[†,‡] Chensheng Lin,[†] and Zhangzhen He[†]

[†]*State Key Laboratory of Structural Chemistry, Fujian Institute of Research on the Structure of Matter, Chinese Academy of Sciences, Fuzhou 350002, People's Republic of China and* [‡]*Graduate School of the Chinese Academy of Sciences, Beijing 100039, People's Republic of China*

Received December 11, 2009

Explorations of the $A^{I}-M^{III}-B^{III}-P^{V}-O$ quinary system under solid-state reactions led to an anhydrous cesium−chromium borophosphate−phosphate and an anhydrous cesium−iron borophosphate, namely, $Cs_2Cr_3(BP_4O_{14})(P_4O_{13})$ (**1**) and $CsFe(BP_3O_{11})$ (**2**). They both feature complicated three-dimensional (3D) frameworks and represent the first examples of borophosphate frameworks with a P−O−P connection. Compound **1** contains a novel anionic borophosphate partial structure $[B(P_2O_7)_2]^{5-}$ with B:P = 1:4 besides an isolated $[P_4O_{13}]^{6-}$ anion. Its 3D structure is composed of a layer of $[CrB(P_2O_7)_2]_n^{2n-}$ and a neutral layer of $[Cr_2(P_4O_{13})]_n$ interconnected with the linking of P−O−Cr, and the Cs ions are located at the space. Compound **2** contains another novel borophosphate anionic unit of $[B(PO_4)(P_2O_7)]^{4-}$ with B:P = 1:3, which further bridges the Fe cations to constitute the whole structure. Both compounds are of high thermal stable and transparent in the range of 0.75−7.1 μm. Magnetic measurements indicate that there exist antiferromagnetic interactions in both compounds.

Introduction

Borophosphates have been a subject of interest for many decades because of their rich structural chemistry and potential applications in sorption and separation, heterogeneous catalysis, photonic technologies, ion exchange, and so on.[1] It is well-known that borates and phosphates all exhibit complex structures[2] and tend to form the polynuclear anionic units.[3] In general, the B atoms reveal two kinds of coordination modes, either triangular or tetrahedral. The BO_3 and BO_4 groups favor condensation via common corners to form polynuclear anionic units including isolated clusters,[4] infinite chains,[5] sheets,[6] and frameworks;[7] however, the PO_4 groups favor condensation via common corners to form different oligomeric units such as P_2O_7, P_3O_{10}, P_4O_{13}, P_6O_{18}, and so on. This general principle can be introduced into borophosphates, which leads to the large group of borophosphates with new condensation patterns of complex anions.

*To whom correspondence should be addressed. E-mail: cwd@fjirsm.ac.cn.

(1) (a) Sevov, S. C. *Angew. Chem.* **1996**, *108*, 2814. *Angew. Chem., Int. Ed. Engl.* **1996**, *36*, 2630. (b) Kniep, R.; Gözel, G.; Eisenmann, B.; Röhr, C.; Asbrand, M.; Kizilyalli, M. *Angew. Chem.* **1994**, *106*, 791. *Angew. Chem., Int. Ed. Engl.* **1994**, *33*, 749. (c) Zhao, D.; Cheng, W.-D.; Zhang, H.; Huang, S.-P.; Xie, Z.; Zhang, W.-L.; Yang, S.-L. *Inorg. Chem.* **2009**, *48*, 6623. (d) Yang, T.; Sun, J.-L.; Li, G.-B.; Eriksson, L.; Zou, X.-D.; Liao, F.-H.; Lin, J.-H. *Chem.—Eur. J.* **2008**, *14*, 7212. (e) Yang, W.-T.; Li, J.-Y.; Pan, Q.-H.; Jin, Z.; Yu, J.-H.; Xu, R.-R. *Chem. Mater.* **2008**, *20*, 4900. (f) Dumas, E.; Debiemme-Chouvy, C.; Sevov, S. C. *J. AM. CHEM. SOC.* **2002**, *124*, 908. (g) Liu, W.; Li, M.-R.; Chen, H.-H.; Yang, X.-X.; Zhao, J.-T. *Dalton Trans.* **2004**, 2847. (h) Menezes, P. W.; Hoffmann, S.; Prots, Y.; Kniep, R. *Z. Anorg. Allg. Chem.* **2009**, *635*, 614. (i) Kniep, R.; SchSfer, G.; Engelhardt, H.; Boy, I. *Angew. Chem.* **1999**, *111*, 3857. *Angew. Chem., Int. Ed.* **1999**, *38*, 3641. (j) Zhang, H. Y.; Chen, Z. X; Weng, L. H.; Zhou, Y. M.; Zhao, D. Y. *Microporous Mesoporous Mater.* **2003**, *57*, 309. (k) Yang, M.; Yu, J. H.; Chen, P.; Li, J. Y.; Fang, Q. R.; Xu, R. R. *Microporous Mesoporous Mater.* **2005**, *87*, 124.

(2) (a) Heller, G. *Top. Curr. Chem.* **1986**, *131*, 39. (b) Haushalter, R. C.; Mundi, L. A. *Chem. Mater.* **1992**, *4*, 31.

(3) (a) Burns, P. C.; Grice, J. D.; Hawthorne, F. C. *Can. Mineral.* **1995**, *33*, 1131. (b) Mercader, R. C.; Terminiello, L. *Phys. Rev. B: Condens. Matter* **1990**, *42*, 25. (c) Cruickshank, D. W. J. *Acta Crystallogr.* **1964**, *17*, 674. (d) Ondik, H. M. *Acta Crystallogr.* **1965**, *18*, 226. (e) Averbuch-Pouchot, M. T. *Acta Crystallogr., Sect. C* **1989**, *45*, 1273.

(4) (a) Salentine, C. G. *Inorg. Chem.* **1987**, *26*, 128. (b) Schubert, D. M.; Visi, M. Z.; Knobler, C. B. *Inorg. Chem.* **2000**, *39*, 2250. (c) Touboul, M.; Penin, N.; Nowogrocki, G. *J. Solid State Chem.* **1999**, *143*, 260. (d) Kong, F.; Jiang, H.-L.; Hu, T.; Mao, J.-G. *Inorg. Chem.* **2008**, *47*, 10611. (e) Kong, F.; Huang, S.-P.; Sun, Z.-M.; Mao, J.-G.; Cheng, W.-D. *J. Am. Chem. Soc.* **2006**, *128*, 7750.

(5) (a) Park, H.; Barbier, J.; Hammond, R. P. *Solid State Sci.* **2003**, *5*, 565. (b) Schubert, D. M.; Alam, F.; Visi, M. Z.; Knobler, C. B. *Chem. Mater.* **2003**, *15*, 866. (c) Yu, Z. T.; Shi, Z.; Jiang, Y. S.; Yuan, H. M.; Chen, J. S. *Chem. Mater.* **2002**, *14*, 1314.

(6) (a) Bubnova, R. S.; Fundamensky, V. S.; Anderson, J. E.; Filatov, S. K. *Solid State Sci.* **2002**, *4*, 87. (b) Emme, H.; Huppertz, H. *Z. Anorg. Allg. Chem.* **2002**, *628*, 2165. (c) Penin, N.; Seguin, L.; Touboul, M.; Nowogrocki, G. *Solid State Sci.* **2002**, *4*, 67. (d) Penin, N.; Touboul, M.; Nowogrocki, G. *J. Solid State Chem.* **2002**, *168*, 316. (e) Penin, N.; Touboul, M.; Nowogrocki, G. *Solid State Sci.* **2003**, *5*, 559.

(7) (a) Harrison, W. T. A.; Gier, T. E.; Stucky, G. D. *Angew. Chem., Int. Ed. Engl.* **1993**, *32*, 724. (b) Huppertz, H.; Von Der Eltz, B. *J. Am. Chem. Soc.* **2002**, *124*, 9376. (c) Huppertz, H.; Heymann, G. *Solid State Sci.* **2003**, *5*, 281. (d) Penin, N.; Seguin, L.; Touboul, M.; Nowogrocki, G. *J. Solid State Chem.* **2001**, *161*, 205. (e) Rowsell, J. L. C.; Taylor, N. J.; Nazar, L. F. *J. Am. Chem. Soc.* **2002**, *124*, 6522.

Published on Web 01/29/2010

Scheme 1. Coordination Modes of the Anion Groups in Compounds **1** and **2**

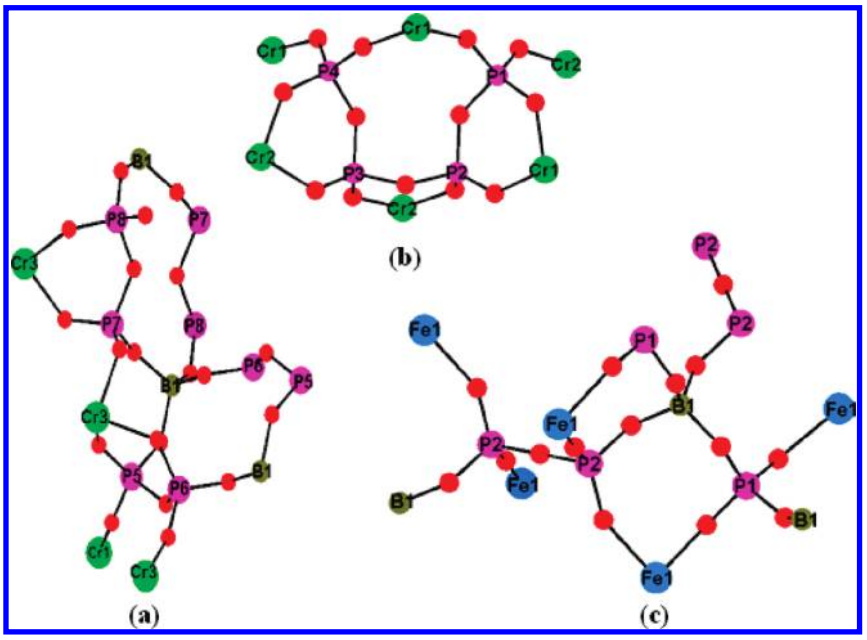

The systematic development of the structural chemistry of the borophosphates has led to a broad spectrum of new borophosphate compounds with quite different anionic partial structures, such as oligomeric units,[8] chains,[9] ribbons,[10] layers,[11] and three-dimensional (3D) frameworks.[12] The borophosphate compounds known to date are systemically classified in terms of reviews by Kniep et al.[13] Disregarding the polyhedra of metal atoms and focusing on the anionic partial structures of borophosphates, which are useful to guide our understanding of borophosphate structures, Kniep et al. concluded a few principles and fundamental building units (FBUs) from the diverse structures. So, there are two main classification criterions of borophosphate compounds. One is the ratio of borate to phosphate in the borophosphate anion. The other is the disassembly of the anionic partial structure into their FBUs.

As is known, most of the borophosphate compounds were synthesized under hydrothermal conditions; hence, their structures usually incorporate water molecules or organic templates, and they are generally not desirable as practical materials. There are rarely reports of anhydrous borophosphate compounds, which might have better chemical and thermal stability than the hydrated phase ones to ensure the feasibility of the industrial applications.[14] Our explorations of new phases in the $Cs-Cr^{III}/Fe^{III}-B^{III}-P^{V}-O$ systems led to two new quinary compounds, namely, $Cs_2Cr_3(BP_4O_{14})(P_4O_{13})$ (**1**) and $CsFe(BP_3O_{11})$ (**2**), with the three types of anionic structures given in Scheme 1. Herein, we report their syntheses, structures, and optical and magnetic properties.

Experimental Section

Materials and Instrumentation. All of the chemicals were analytically pure from commercial sources and were used without further purification. $NH_4H_2PO_4$, H_3BO_3, Fe_2O_3, Cr_2O_3, and Cs_2CO_3 were purchased from the Shanghai Reagent Factory. Single crystals of the title compounds were both selected for indexing and intensity data collection on a Rigaku Mercury CCD diffractometer at a temperature of 293 K. The structures were solved by direct methods and refined anisotropically using *SHELXS-97*. Microprobe elemental analyses were performed by using a field-emission scanning electron microscope (JSM6700F) equipped with an energy-dispersive X-ray spectrometer (Oxford INCA). The X-ray diffraction (XRD) patterns were recorded on a PANalytical X'Pert PRO diffractometer with Cu Kα radiation (40 kV and 40 mA) in the continuous scanning mode. The 2θ scan range was from 5° to 70° in steps of 0.017° with a collection time of 10 s per step. Thermogravimetric analyses (TGA) and differential thermal analyses (DTA) were carried out with a NETZSCH STA 449C unit under an air atmosphere. The samples were placed in Al_2O_3 crucibles and heated from 35 to 1200 °C at a rate of 10.0 °C min^{-1}. Fourier transform infrared spectroscopy spectra were recorded on a Magna 750 as KBr pellets in the range of 4000−400 cm^{-1}. The UV−vis absorption spectrum was measured at room temperature with a Perkin-Elmer Lambda 900 UV−vis spectrophotometer in the wavelength range of 190−1200 nm. A $BaSO_4$ plate was used as a standard (100% reflectance). Magnetic susceptibility

(8) (a) Boy, I.; Cordier, G.; Kniep, R. *Z. Kristallogr.—New Cryst. Struct.* **1998**, *213*, 29. (b) Boy, I.; Cordier, G.; Eisenmann, B.; Kniep, R. *Z. Naturforsch. B* **1998**, *53*, 165. (c) Boy, I.; Cordier, G.; Kniep, R. *Z. Naturforsch. B* **1998**, *53*, 1440. (d) Hauf, C.; Boy, I.; Kniep, R. *Z. Kristallogr.—New Cryst. Struct.* **1999**, *214*, 3.

(9) (a) Hauf, C.; Friedrich, T.; Kniep, R. *Z. Kristallogr.* **1995**, *210*, 446. (b) Hauf, C.; Kniep, R. *Z. Kristallogr.* **1996**, *211*, 705. (c) Hauf, C.; Kniep, R. *Z. Kristallogr.* **1996**, *211*, 707. (d) Hauf, C.; Kniep, R. *Z. Kristallogr.—New Cryst. Struct.* **1997**, *212*, 313. (e) Boy, I.; Hauf, C.; Kniep, R. *Z. Naturforsch. B* **1998**, *53*, 631. (f) Kniep, R.; Boy, I.; Engelhardt, H. *Z. Anorg. Allg. Chem.* **1999**, *625*, 1512.

(10) (a) Kniep, R.; Will, H. G.; Boy, I.; Röhr, C. *Angew. Chem.* **1997**, *109*, 1052. *Angew. Chem., Int. Ed. Engl.* **1997**, *36*, 1013. (b) Boy, I.; Kniep, R. *Z. Naturforsch. B* **1999**, *54*, 895.

(11) Kniep, R.; Engelhardt, H. *Z. Anorg. Allg. Chem.* **1998**, *624*, 1291.

(12) Hauf, C.; Kniep, R. *Z. Naturforsch. B* **1997**, *52*, 1432.

(13) (a) Kniep, R.; Engelhardt, H.; Hauf, C. *Chem. Mater.* **1998**, *10*, 2930. (b) Ewald, B.; Huang, Y. X.; Kniep, R. *Z. Anorg. Allg. Chem.* **2007**, *633*, 1517. (c) Ruchkina, E. A.; Belokoneva, E. L. *Russ. J. Inorg. Chem.* **2003**, *48*, 1812. (d) Ewald, B.; Prots, Y.; Menezes, P.; Natarajan, S.; Zhang, H.; Kniep, R. *Inorg. Chem.* **2005**, *44*, 6431.

(14) (a) Kniep, R.; Gozel, G.; Eisenmann, B.; Röhr, C.; Asbrand, M.; Kizilyalli, M. *Angew. Chem., Int. Ed. Engl.* **1994**, *33*, 791. (b) Xiong, D.-B.; Chen, H.-H.; Yang, X.-X.; Zhao, J.-T. *J. Solid State Chem.* **2007**, *180*, 233. (c) Bontchev, R. P.; Sevov, S. C. *Inorg. Chem.* **1996**, *35*, 6910. (d) Ehrenberg, H.; Laubach, S.; Schmidt, P. C.; McSweeney, R.; Knappa, M.; Mishra, K. C. *J. Solid State Chem.* **2006**, *179*, 968. (e) Mi, J.-X.; Zhao, J.-T.; Mao, S.-Y.; Huang, Y.-X.; Engelhardt, H.; Kniep, R. *Z. Kristallogr.—New Cryst. Struct.* **2000**, *215*, 201.

measurements for two compounds were performed with a PPMS-9T magnetometer at 1000 or 10 000 Oe in the temperature range 2−300 K. The raw data were corrected for the susceptibility of the container and the diamagnetic contributions of the sample using Pascal constants.

Synthesis of $Cs_2Cr_3(BP_4O_{14})(P_4O_{13})$ (1). Compound **1** was synthesized by a solid-state reaction. A powder mixture of 0.81 g of Cs_2CO_3, 0.073 g of Cr_2O_3, 0.77 g of H_3BO_3, and 1.01 g of $NH_4H_2PO_4$ was first ground in an agate mortar and then transferred to a platinum crucible. The sample was gradually heated in air at 573 K for 6 h to decompose H_3BO_3 and $NH_4H_2PO_4$ and finally heated at 1323 K for 24 h. The intermediate product was slowly cooled to 1073 K at a rate of 2 K h^{-1}, where it was kept for 10 h and then quenched to room temperature. Some bottle-green crystals were selected carefully from the solidified flux with hot water for the single-crystal detection. After structural analysis, a green crystalline powder sample of **1** was then obtained quantitatively by the reaction of a mixture of Cs_2CO_3, Cr_2O_3, H_3BO_3, and $NH_4H_2PO_4$ in a molar ratio of 2:3:2:16 at 1123 K for 30 h. The purity of compound **1** was confirmed by a powder XRD study (Figure S1a in the Supporting Information).

Synthesis of $CsFe(BP_3O_{11})$ (2). The synthesis of single crystals of compound **2** was carried out using a powder mixture of 0.17 g of Cs_2CO_3, 0.05 g of Fe_2O_3, 0.50 g of H_3BO_3, and 0.63 g of $NH_4H_2PO_4$ in a molar ratio corresponding to Cs:Fe:B:P = 2:1:20:12; the excess amounts of $NH_4H_2PO_4$ and H_3BO_3 are present to promote crystal growth. The mixture was first ground in an agate mortar and then introduced into a platinum crucible. The crucible was heated at 573 K for 1 day, then heated for 2 days at 1123 K, cooled to 923 K at a rate of 3 K h^{-1}, and finally quenched to room temperature. Some transparent block crystals were selected carefully from the sintered product with hot water. Subsequently, a pure powder sample of **2** was prepared quantitatively by the reaction of a mixture of Cs_2CO_3, Fe_2O_3, H_3BO_3, and $NH_4H_2PO_4$ in a molar ratio of 1:1:2:6 at 1153 K. The purity of the powder sample of compound **2** was confirmed by a powder XRD study (Figure S1b in the Supporting Information).

Single-Crystal Structure Determination. Single crystals of the title compounds were both selected for indexing and intensity data collection on a Rigaku Mercury CCD diffractometer at a temperature of 293 K. Absorption corrections by the multiscan method were applied for both of them,[15a] and then both structures were solved by direct methods, then refined on F^2 by a full-matrix least-squares method, and performed in the *SHELXL/PC* programs.[15b] All atoms were refined with anisotropic thermal parameters. Crystallographic data and structural refinements for the two title compounds are summarized in Table 1. The atomic coordinates are listed in Table S1 (see the Supporting Information), and important bond distances are listed in Table S2 (see the Supporting Information). The final refined solutions obtained were checked with the *ADDSYM* algorithm in the program *PLATON*,[16] and no higher symmetry was found. In order to confirm the chemical composition of the compounds, we do microprobe elemental analyses of the single crystals, indicating the presence of Cs, Cr, and P elements in a molar ratio of 4.01:5.82:17.02 in compound **1** and Cs, Fe, and P elements in a molar ratio of 2.14:1.98:7.62 in compound **2**. Because samples were unpolished and X-ray corrections may be approximate especially for light elements, the energy-dispersive X-ray spectrometry results were in agreement with those from single-crystal X-ray structural analyses. ICSD nos. 420498 and 420497 contain the supplementary crystallographic data for this paper. The data can be obtained from Fachinformationszentrum Karlsruhe, 76344 Eggenstein-Leopoldshafen, Germany [fax (49) 7247-808-666; e-mail crysdata@fiz-karlsruhe.de].

Table 1. Crystal Data and Structural Refinements for Compounds **1** and **2**

	1	**2**
formula	$Cs_2Cr_3(BP_4O_{14})(P_4O_{13})$	$CsFe(BP_3O_{11})$
fw	1112.39	468.48
space group	$P2(1)/c$ (No. 14)	*Pnma* (No. 62)
a, Å	14.7918(14)	8.5375(7)
b, Å	15.8190(15)	12.7829(12)
c, Å	9.7037(8)	8.3346(5)
α, deg	90	90
β, deg	92.450(6)	90
γ, deg	90	90
V, Å^3	876.9 (2)	909.59(13)
Z	4	4
D_{calcd}, g cm^{-3}	3.257	3.434
μ, mm^{-1}	5.266	6.185
GOF on F^2	1.051	1.083
R1, wR2 [$I > 2\sigma(I)$][a]	0.0414, 0.0945	0.0210, 0.0470
R1, wR2 (all data)	0.0485, 0.0992	0.0214, 0.0471

[a] $R1 = \sum||F_o| - |F_c||/\sum|F_o|$, $wR2 = \{\sum w[(F_o)^2 - (F_c)^2]^2/\sum w[(F_o)^2]^2\}^{1/2}$.

Results and Discussion

Solid-state reactions of Cs_2CO_3, H_3BO_3, $NH_4H_2PO_4$, and Cr_2O_3 (or Fe_2O_3) afford an anhydrous cesium−chromium borophosphate−phosphate, $Cs_2Cr_3(BP_4O_{14})(P_4O_{13})$ (**1**), and an anhydrous cesium−iron borophosphate, $CsFe(BP_3O_{11})$ (**2**). The two title compounds feature novel 3D structures with undiscovered borophosphate anionic groups of $[B(P_2O_7)_2]^{5-}$ and $[B(PO_4)(P_2O_7)]^{4-}$ for **1** and **2**, respectively.

Structural Descriptions. The asymmetric unit of compound **1** consists of two Cs ions, three Cr ions, and two types of complex anionic groups, $[P_4O_{13}]^{6-}$ and $[B(P_2O_7)_2]^{5-}$. All of the atoms represent independent crystallographic sites. Each B atom is tetrahedrally coordinated by four O atoms, forming a BO_4 tetrahedron geometry with B−O bond lengths ranging from 1.454(6) to 1.472(6) Å. Each P atom is also coordinated by four O atoms in a tetrahedral geometry with P−O bond distances ranging from 1.476(3) to 1.625(3) Å. Two types of condensation of $[PO_4]^{3-}$ groups lead to two anionic units, namely, $[P_4O_{13}]^{6-}$ and $[P_2O_7]^{3-}$, which display different conjunctive modes (Scheme 1a,b) in compound **1**. The P−O bond distances are listed in Table S2 of the Supporting Information. The shortest P−O distances are found from the P−O−Cr linking, varying from 1.476(3) to 1.510(4) Å, the distances of the P−O bonds within the P−O−B linking are in the range from 1.531(3) to 1.543(3) Å, and the longest distances of the P−O bonds within the P−O−P linking are in the range from 1.540(4) to 1.625(3) Å. The anion of $[P_4O_{13}]^{6-}$ has never been observed in any borophosphate or borophosphate−phosphate compounds. The $[BO_4]^{5-}$ and $[P_2O_7]^{3-}$ groups are connected to each other alternatively via B−O−P−O−P−O−B linking, leading to a 1D anionic chain of $[B(P_2O_7)_2]_n^{5n-}$ along the c axis, as shown in Figure 1.

Each Cr atom is six-coordinated by six O atoms in a octahedral geometry, with Cr−O bond distances ranging from 1.937(3) to 1.994(3) Å. The CrO_6 octahedra are further connected with two types of anionic groups, $[P_4O_{13}]^{6-}$ and $[B(P_2O_7)_2]^{5-}$, to form a 3D framework of $[Cr_3BP_8O_{27}]^{2-}$ anions. The Cr3 ions are connected with

(15) (a) *CrystalClear*, version 1.3.5; Rigaku Corp.: Woodlands, TX, **1999**. (b) Sheldrick, G. M. *SHELXTL, Crystallographic Software Package, SHELXTL*, version 5.1; Bruker-AXS: Madison, WI, **1998**.

(16) Spek, A. L. *J. Appl. Crystallogr.* **2003**, *36*, 7.

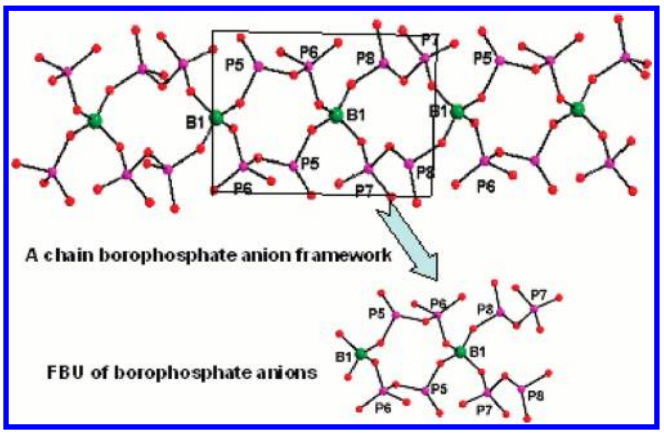

Figure 1. $[B(P_2O_7)_2]_n^{5n-}$ chain borophosphate anion framework of compound **1** and its FBU $[B(P_2O_7)_2]_2^{10-}$. The P, B, and O atoms are represented by pink, green, and red circles, respectively.

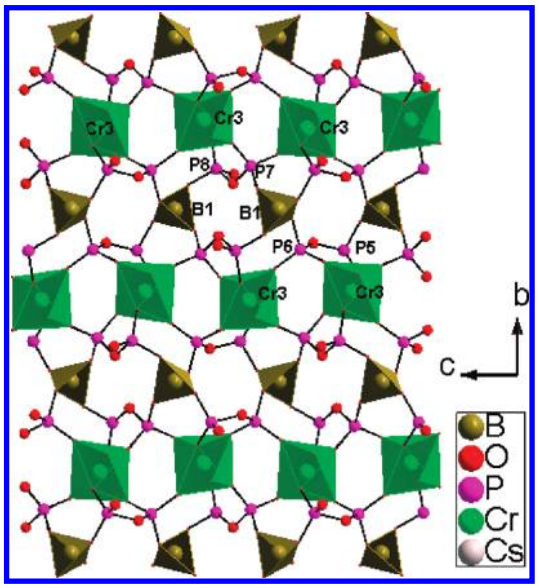

Figure 2. 2D layer of $[CrB(P_2O_7)_2]_n^{2n-}$ anions along the *a* axis. The Cs, Cr, P, B, and O atoms are represented by gray, green, pink, brown, and red circles, respectively.

$[B(P_2O_7)_2]^{5-}$ anions into a two-dimensional (2D) layer of $[CrB(P_2O_7)_2]_n^{2n-}$ anions along the *a* axis (Figure 2). The remaining Cr1 and Cr2 ions are bridging with the anion of $[P_4O_{13}]^{6-}$ to form a neutral layer of $[Cr_2(P_4O_{13})]_n$ (Figure 3). The above-mentioned two types of layers are further interconnected by the P−O−Cr linking to form a 3D framework. In connectivity terms, the structure can be written as $\{[CrB(P_2O_7)_2]_n^{2n-}\cdots[Cr_2(P_4O_{13}]_n\}^{2n-}$ with the charge balance maintained by the $Cs1^+$ and $Cs2^+$ cations (Figure 4). It is worth mentioning that the $[P_4O_{13}]^{6-}$ anion acts as a hexadentated mental linker; it chelates in bidentate order with four Cr^{3+} cations and shares two qof the rest of the O atoms with two CrO_6 octahedra; hence, the $[P_4O_{13}]^{6-}$ anion connects six neighboring CrO_6 octahedra to form a neutral layer of $[Cr_2(P_4O_{13})]_n$, and that is why the $[P_4O_{13}]^{6-}$ group in compound **1** can be ignored when we talk about the borophosphate partial structure. It is worth comparing the structures of compound **1** and another borophosphate−phosphate compound, $Na_8[Cr_4B_{12}P_8O_{44}(OH)_4][P_2O_7]\cdot nH_2O$.[1d] $Na_8[Cr_4B_{12}P_8O_{44}(OH)_4][P_2O_7]\cdot nH_2O$ represents the first borate-rich

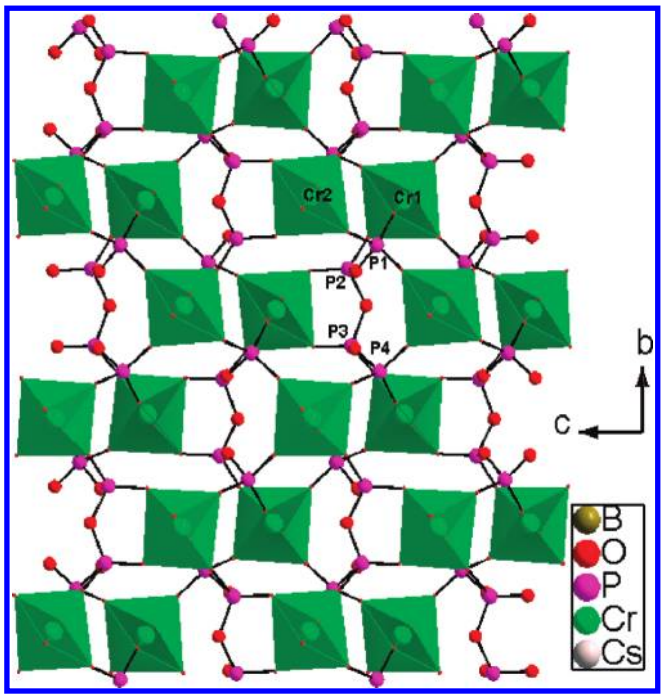

Figure 3. Neutral layer of $[Cr_2(P_4O_{13})]_n$. The Cs, Cr, P, B, and O atoms are represented by gray, green, pink, brown, and red circles, respectively.

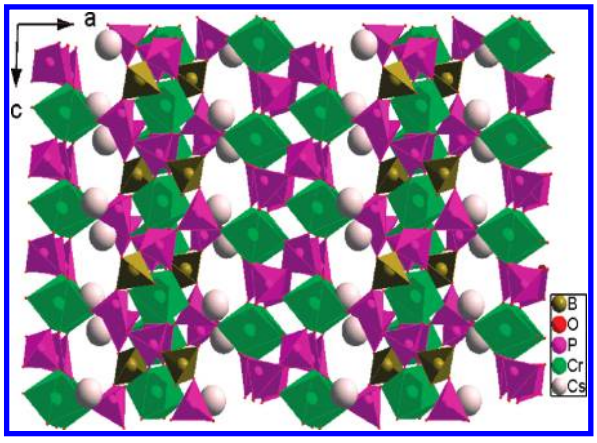

Figure 4. View of the structure of compound **1** along the *b* axis. The Cs, Cr, P, B, and O atoms are represented by gray, green, pink, brown, and red circles, respectively.

borophosphate adopting a spherical cage framework structure composed of CrO_6, PO_4, BO_4, and BO_3 polyhedra, and it features a 3D borophosphate partial framework structure, represented as $^3_\infty[B_3P_2O_{11}(OH)]$, in which the $[P_2O_7]^{4-}$ anionic group is also ignored. The borophosphate partial framework structures of the two borophosphate−phosphate compounds are different. From the above discussions, we know that compound **1** features a 1D anionic chain of $[B(P_2O_7)_2]_n^{5n-}$ along the *c* axis, whereas the compound $Na_8[Cr_4B_{12}P_8O_{44}(OH)_4][P_2O_7]\cdot nH_2O$ features a 3D borophosphate partial framework structure.

The crystal structure of compound **2** contains 17 atoms, 15 atoms belonging to the borophosphate anionic framework (1 B, 3 P, and 11 O atoms) and 1 Fe atom and 1 Cs atom playing the roles of charge balance. Compared with compound **1**, which features a chain borophosphate anionic framework as mentioned above (Figure 1), there

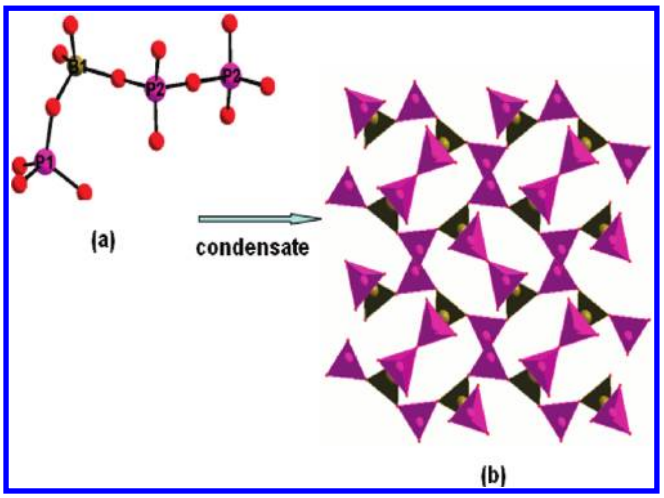

Figure 5. Anion unit of $[BP_3O_{11}]^{4-}$ (a) and the 3D anion framework of $\{BP_3O_{11}\}_n^{4n-}$ (b) of compound **2**.

is a complex 3D borophosphate anionic framework in compound **2**, which is built by the borophosphate anionic group of $[B(PO_4)(P_2O_7)]^{4-}$ (Figure 5a). The group is composed of a borate tetrahedron branched by one PO_4 group and one P_2O_7 group via corner-sharing, with the B−O bond distances ranging from 1.445(5) to 1.463(6) Å. The $[B(PO_4)(P_2O_7)]^{4-}$ anionic group arrayed via corner-sharing to form a complex 3D anion structure (Figure 5b), then the borophosphate framework was further connected by corner-sharing with iron octahedra to form a novel 3D open framework, and the Cs cations are located in the space and serve in charge balance. As shown in Figure 6, the Fe^{3+} cations are six-coordinated by four $[P_2O_7]^{4-}$ groups and two $[PO_4]^{3-}$ anions in a unidentate fashion. The Fe−O bond distances range from 2.290(4) to 2.482(4) Å (Table S2 in the Supporting Information). In the novel borophosphate anionic group of $[B(PO_4)(P_2O_7)]^{4-}$, the $[P_2O_7]^{4-}$ anion is hexadentate, in which four O atoms bridge with a Fe^{3+} cation in a unidentate fashion and the other two O atoms share the corners with two BO_4 tetrahedra, and the $[PO_4]^{3-}$ anion is tetradentate, with two O atoms connecting to two Fe^{3+} cations and the other two O atoms sharing corners with two BO_4 tetrahedra (Scheme 1c). The shortest P−O distances are found from the P−O−Fe linking, varying from 1.467(3) to 1.512(2) Å, the distances of the P−O bonds within the P−O−B linking are in the range from 1.534(3) to 1.545(2) Å, and the longest distance of the P−O bonds within the P−O−P linking is 1.5464(8) Å, which is comparable to compound **1** mentioned above.

The 3D inorganic network of **2** can also be viewed as built from the $[FeP_2O_7]_n^{n-}$ layer based on corner-sharing FeO_6 octahedra and the $[P_2O_7]^{4-}$ groups interconnected by the 1D chain of $[BPO_4]_n$. Each FeO_6 octahedron is connected to four neighboring $[P_2O_7]^{4-}$ groups, and also each $[P_2O_7]^{4-}$ group is connected to four neighboring FeO_6 octahedra via the Fe−O−P linking into a 2D layer parallel to the *ac* plane (Figure 6a). In the view of topology, both the FeO_6 octahedron and the $[P_2O_7]^{4-}$ group are four-connector; hence, the layer can be considered as a (4,4)-connected layer. The 1D chain of $[BPO_4]_n$ is built by the $[BO_4]^{5-}$ and $[PO_4]^{3-}$ groups linked alternately via corner-sharing (Figure 6b). Adjacent layers of $[FeP_2O_7]_n^{n-}$ are interconnected by the 1D chain of $[BPO_4]_n$ into a 3D network with eight-membered-ring tunnels formed by two FeO_6 octahedra, five PO_4 tetrahedra, and one BO_4 tetrahedron along the *a* axis (Figure 6c), and the Cs cations are located at the eight-membered-ring tunnels (Figure 6d).

It is also worth comparing the structures of the title compound **2** with other M^IM^{III} borophosphates. As is known, a series of hydrous M^IM^{III} borophosphates have recently been investigated systematically in the hydrothermal method (Table 2), in which five types of borophosphate compounds were already observed, namely, $M^IM^{III}[BP_2O_8(OH)]$ ($P2_1/c$),[17] $M^IM^{III}[BP_2O_7(OH)_3]$ ($C2/c$),[18] $M^IM^{III}[BP_2O_8(OH)]$ ($P\bar{1}$),[19] and $M^IM^{III}[B_2P_3O_{11}(OH)_3]$ (*Pnna*).[20] $M^IM^{III}[BP_2O_8(OH)]$ ($P2_1/c$),[17] $M^IM^{III}[BP_2O_7(OH)_3]$ ($C2/c$),[18] and $M^IM^{III}[BP_2O_8(OH)]$ ($P\bar{1}$)[19] all consist of almost the same borophosphate anions $[BP_2O_x]$ ($x = 9, 10$) with B:P = 1:2. For M^IM^{III} $[B_2P_3O_{11}(OH)_3]$ (*Pnna*),[20] its anionic partial structure $[B_2P_3O_{11}(OH)_3]^{4-}$ is built of a central borate tetrahedron open-branched by two $(OH)PO_3$ tetrahedra and cyclobranched by one PO_4 tetrahedron and a trigonal-planar $(OH)BO_2$. Unlike the M^IM^{III} borophosphates that we mentioned above, the title compound **2** features a novel 3D open framework with undiscovered anionic borophosphate groups of $[B(PO_4)(P_2O_7)]^{4-}$ with B:P = 1:3. Additionally, as far as we know, the M^IM^{III} borophosphate frameworks are featured by two kinds of anionic partial structures, oligomeric units, and one-dimensional (1D) chains (Table 2). From the discussion above, we know that there is a complex 3D borophosphate open framework built by a novel borophosphate anionic group of $[B(PO_4)(P_2O_7)]^{4-}$ in compound **2**. So, compound **2** is the first compound containing a 3D borophosphate open framework in the mixed-metal M^IM^{III} borophosphates.

Borophosphate Partial Structure. To further understand the structures, we have employed Kniep et al.'s concept and the nomenclature of borophosphate FBUs[13]

(17) (a) Engelhardt, H.; Borrmann, H.; Kniep, R. *Z. Kristallogr.—New Cryst. Struct.* **2000**, *215*, 203. (b) Kniep, R.; Koch, D.; Hartmann, T. *Z. Kristallogr.—New Cryst. Struct.* **2002**, *217*, 186. (c) Mi, J. X.; Zhao, J. T.; Huang, Y. X.; Deng, J. F.; Borrmann, H.; Kniep, R. *Z. Kristallogr.—New Cryst. Struct.* **2002**, *217*, 171. (d) Mi, J. X.; Huang, Y. X.; Deng, J. F.; Borrmann, H.; Zhao, J. T.; Kniep, R. *Z. Kristallogr.—New Cryst. Struct.* **2002**, *217*, 169. (e) Mi, J. X.; Borrmann, H.; Huang, Y. X.; Mao, S. Y.; Zhao, J. T.; Kniep, R. *Z. Kristallogr.—New Cryst. Struct.* **2003**, *218*, 171. (f) Mi, J. X.; Borrmann, H.; Mao, S. Y.; Huang, Y. X.; Zhang, H.; Zhao, J. T.; Kniep, R. *Z. Kristallogr.—New Cryst. Struct.* **2003**, *218*, 17. (g) Kniep, R.; Boy, I.; Engelhardt, H. *Z. Anorg. Allg. Chem.* **1999**, *625*, 1512. (h) Engelhardt, H.; Kniep, R. *Z. Kristallogr.—New Cryst. Struct.* **1999**, *214*, 443. (i) Mao, S. Y.; Li, M.-R.; Wei, Z.-B.; Mi, J.-X.; Zhao, J.-T. *Wuji Huaxue Xuebao* **2004**, *20*, 53.

(18) (a) Koch, D.; Kniep, R. *Z. Kristallogr.—New Cryst. Struct.* **1999**, *214*, 441. (b) Huang, Y. X.; Mao, S. Y.; Mi, J. X.; Wei, Z. B.; Zhao, J. T.; Kniep, R. *Z. Kristallogr.—New Cryst. Struct.* **2001**, *216*, 15. (c) Mi, J. X.; Huang, Y. X.; Mao, S. Y.; Borrmann, H.; Zhao, J. T.; Kniep, R. *Z. Kristallogr.—New Cryst. Struct.* **2002**, *217*, 167. (d) Huang, Y. X.; Mi, J. X.; Mao, S. Y.; Wei, Z. B.; Zhao, J. T.; Kniep, R. *Z. Kristallogr.—New Cryst. Struct.* **2002**, *217*, 7. (e) Zhang, L. R.; Zhang, H.; Borrmann, H.; Kniep, R. *Z. Kristallogr.—New Cryst. Struct.* **2002**, *217*, 477. (f) Boy, I.; Cordier, G.; Eisenmann, B.; Kniep, R. *Z. Naturforsch. B: Chem. Sci.* **1998**, *53*, 165.

(19) (a) Mao, S. Y.; Li, M. R.; Huang, Y. X.; Mi, J. X.; Wei, Z. B.; Zhao, J. T.; Kniep, R. *Z. Kristallogr.—New Cryst. Struct.* **2002**, *217*, 3. (b) Menezes, P. W.; Hoffmann, S.; Prots, Yu.; Kniep, R. *Z. Kristallogr.—New Cryst. Struct.* **2006**, *221*, 251. (c) Menezes, P. W.; Hoffmann, S.; Prots, Yu.; Kniep, R. *Z. Kristallogr.—New Cryst. Struct.* **2006**, *221*, 253.

(20) Menezes, P. W.; Hoffmann, S.; Prots, Yu.; Kniep, R. *Inorg. Chem.* **2007**, *18*, 7503.

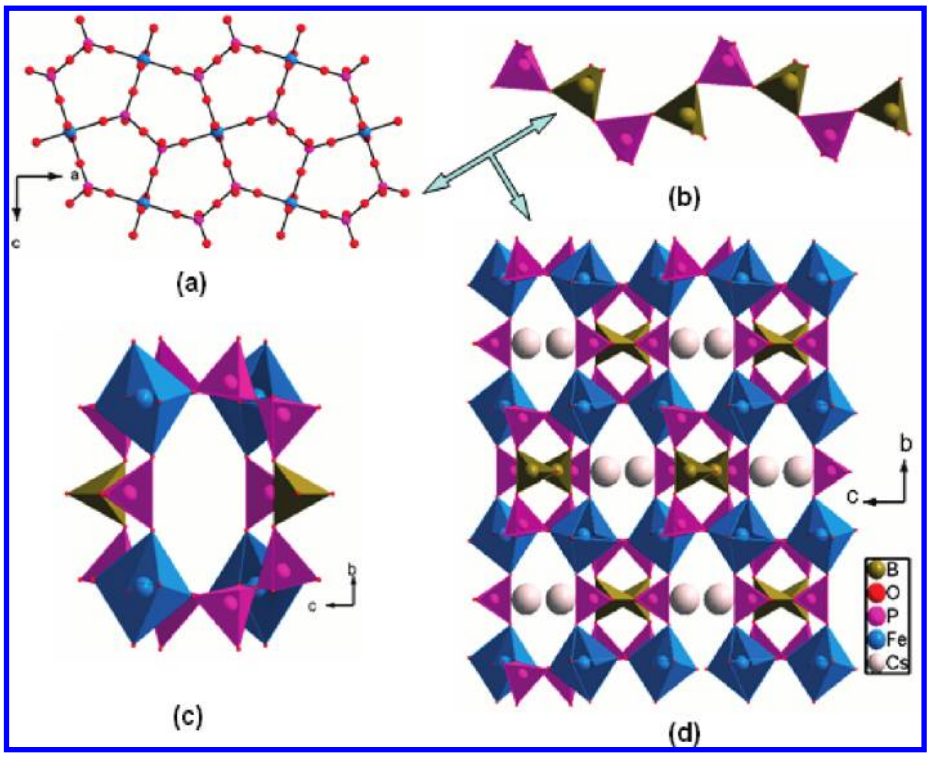

Figure 6. $[FeP_2O_7]_n^{n-}$ layer (a), the 1D chain of $[BPO_4]_n$ (b), the eight-membered ring (two FeO_6, five PO_4, and one BO_4) (c), and view of the structure of compound **2** along the *a* axis (d). The Cs, Fe, P, B, and O atoms are represented by gray, blue, pink, brown, and red circles, respectively.

Table 2. Structure Table for the Known Mixed-Metal M^IM^{III} Borophosphates

compound	space group	borophosphate anion	borophosphate anion frameworks	ref
$AM^{III}[BP_2O_7(OH)_3]$ (A = Na, K; M^{III} = V, Fe, Al, Ga, In)	$C2/c$ (No. 15)	$[BP_2O_{10}]$	oligomers	18
$AM^{III}[BP_2O_8(OH)]$ (A = NH_4^+, K, Rb; M^{III} = Sc, Fe, In)	$P\bar{1}$ (No. 2)	$[BP_2O_9]$	oligomers	19
$AM^{III}[BP_2O_8(OH)]$ (A = NH_4^+, Rb, Cs; M^{III} = V, Fe ($Fe_{0.53}V_{0.47}$), Al, Ga)	$P2_1/c$ (No. 14)	$[BP_2O_9]$	chains	17
$CsSc[B_2P_3O_{11}(OH)_3]$	*Pbnn* (No. 52)	$[B_2P_3O_{14}]$	oligomers	20

to analyze the borophosphate partial structures of the two title compounds. In Kniep et al.'s description, the transition metal can be ignored; thus, one can focus mainly on the borophosphate partial structures. As mentioned above, there are two main classification criteria of borophosphate compounds: one is the ratio of borate to phosphate in the borophosphate anion, and the other one is the disassembly of the anionic partial structure into their FBUs. The $[P_4O_{13}]^{6-}$ group in compound **1** is an isolated phosphate group that can be ignored, so the FBU of the borophosphate partial structure of compound **1** is $[B(P_2O_7)_2]_2^{10-}$ with B:P = 1:4, whereas the FBU of compound **2** is $[B(PO_4)(P_2O_7)]^{4-}$ with B:P = 1:3.

As is known, in all of the various structures of borophosphate compounds, the P−O−P connection has not been observed within the borophosphate anions, and the borophosphate anions with B:P ratios of less than or equal to 1:4 have not been found with additional phosphate units—isolated or condensed—remain isolated in the crystal structures to date.[13] It is concluded that a possible explanation for missing P−O−P connections can be found in Pauling's fourth rule.[13,21] However, with the synthesis of **1** and **2**, we have now found the existence of the P−O−P linker within borophosphate anionic partial structures of $[B(P_2O_7)_2]^{5-}$ and $[B(PO_4)(P_2O_7)]^{4-}$ and largely extended the chemical diversity of borophosphates. Hence, we consider that the two title compounds represent the first examples with the P−O−P connection within the borophosphate anions, which it is completely unexpected and spectacular.

Thermal Analysis. TGA indicated that compounds **1** and **2** are thermally stable up to high temperatures. For compound **1**, there is no obvious step of weight loss before 1200 °C in the TGA curve, which is also confirmed by the DTA curve (Figure S2a in the Supporting Information). Compound **2** exhibits only one main step of weight loss, and the total weight loss is 2.1% at 1200 °C. The weight loss corresponds to the decomposition of the compound. The final residue was not characterized because of its melting with the Al_2O_3 crucible under such high temperatures. The DTA trace for **2** also exhibits an endothermic peak at 950 °C on the heating curve (Figure S2b in the Supporting Information). Thermal analysis experiments of compound **1** show higher thermal stability than compound **2**; it is expected that the lower the ratio of borate to phosphate, the higher the thermal stability. It is interesting to mention that the B atoms in the two title compounds are surrounded by four O atoms and then further connected by the P atoms to form the B−O−P linker. The anhydrous borophosphates in which the O atoms around

(21) Pauling, L. *J. Am. Chem. Soc.* **1929**, *51*, 1010.

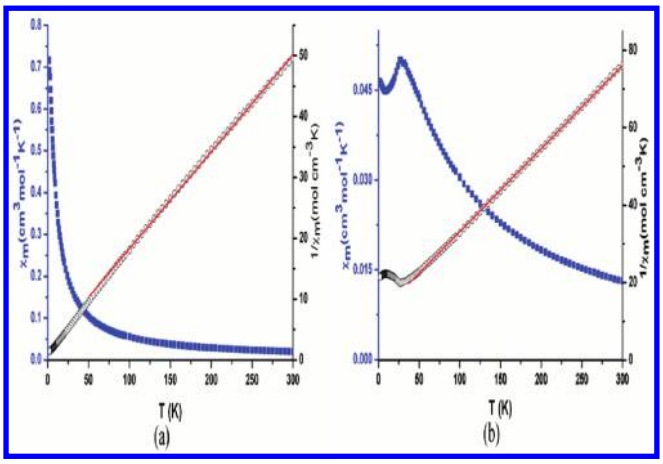

Figure 7. $1/\chi$ vs T and χ vs T plots for **1** (a) and **2** (b). The red lines represent the linear fits of the data according to the Curie−Weiss law.

the B atoms are all connected by the P atoms have been proven to have high thermal stability, such as $KMBP_2O_8$ (M = Sr, Ba),[1c] $Sr_6BP_5O_{20}$,[14d] $Cr_2BP_3O_{12}$,[14e] and so on.

Optical Properties. UV absorption spectra of compounds **1** and **2** show little absorption in the ranges of 750−1200 nm (0.75−1.2 μm) and 400−1200 nm (0.4−1.2 μm), respectively (Figure S3 in the Supporting Information). IR studies indicate that both compounds are transparent in the range of 4000−1400 cm^{-1} (2.5−7.1 μm) (Figure S4 in the Supporting Information). IR spectra of the two title compounds display features similar to those of other metal borophosphates.[1c] Stretching and bending frequencies of the B−O and P−O groups are observed up to 1400 cm^{-1}. The bands at 889, 922, 989, 1023, 1048, 1096, 1123, 1148, 1208, 1257, and 1306 cm^{-1} for **1** and at 873, 939, 992, 1058, 1107, 1190, and 1243 cm^{-1} for **2** are due to the asymmetric and symmetric stretching of B−O in BO_4 and P−O in PO_4, whereas the bands at 446, 481, 508, 527, 558, 575, 612, 642, 674, 742, and 806 cm^{-1} for **1** and at 446, 504, 532, 560, and 632 cm^{-1} for **2** are the out-of-plane bending of B−O in BO_4 or P−O in PO_4. Hence, both compounds are transparent in the range of 0.75−7.1 μm.

Magnetic Properties. The magnetic susceptibilities of compound **1** were measured at a field of 1000 Oe over a temperature range of 2−300 K. Figure 7a shows that the temperature dependences of the magnetic susceptibility for polycrystalline compound **1** Curie−Weiss fit to the high-temperature susceptibility data yields Curie constant C = 6.06(9) emu K mol^{-1} and Weiss constant θ = −7.48(8) K, indicating that a considerably stronger antiferromagnetic couple dominates the exchange between Cr^{III} centers. The effective magnetic moment of Cr^{3+} ions in the system is calculated to be 4.02(3) μ_B, which is a little larger than the value 3.87(3) μ_B obtained by Cr^{3+} ($S = {}^3/_2$) ions, indicating that Cr^{3+} ions have a high spin state and a small orbital moment contribution of Cr^{3+} in the oxygen octahedral environment. The direct-current magnetic properties of compound **2** were measured in the temperature range of 2−300 K at an applied magnetic field of 10 000 Oe. Figure 7b shows the temperature dependences of the magnetic susceptibility for polycrystalline compound **2**. A sharp peak is observed at 28.0 K, indicating the onset of antiferromagnetic ordering. Above 30 K, the susceptibility increases with decreasing temperature, a typical Curie−Weiss behavior, giving the Curie constant C = 4.66(4) emu K mol^{-1} and Weiss constant θ = −54.80(9) K. The effective magnetic moment of Fe^{3+} ions in the system is calculated to be 6.10(4) μ_B, which is larger than the value 5.91(6) μ_B obtained by Fe^{3+} ($S = {}^5/_2$) ions, indicating that Fe^{3+} ions have a high spin state and a small orbital moment contribution of Fe^{3+} in the oxygen octahedral environment. Also, the negative Weiss temperature indicates that a considerably stronger antiferromagnetic couple dominates the exchange between Fe atoms. Figure S5 (see the Supporting Information) shows magnetization (M) as a function of the applied field (H) at T = 2 K. A linear increase in the magnetization is observed for compound **2**, agreeing with an antiferromagnetic ordering below 28.0 K.

Conclusion

In summary, a novel anhydrous cesium−chromium borophosphate−phosphate and a novel anhydrous cesium−iron borophosphate have been successfully isolated by solid-state reactions. With the synthesis of **1** and **2**, we have now found the existence of the P−O−P linker within borophosphate partial structures, which largely extends the chemical diversity of borophosphates. **1** contains a novel borophosphate partial structure $[B(P_2O_7)_2]^{5-}$ with B:P = 1:4 besides isolated $[P_4O_{13}]^{6-}$, whereas **2** also contains another novel borophosphate anionic unit of $[B(PO_4)(P_2O_7)]^{4-}$ with B:P = 1:3. The 3D inorganic network of compound **1** also can be viewed as two types of layers, $[CrB(P_2O_7)_2]_n^{2n-}$ and $[Cr_2(P_4O_{13})]_n$, further interconnected through the P−O−Cr linker to form a 3D open framework, with the charge balance maintained by the Cs^+ cations. In compound **2**, the 3D inorganic network can be viewed as built from the $[FeP_2O_7]_n^{n-}$ layer interconnected by the 1D chain of $[BPO_4]_n$, and also the Cs^+ cations maintained the charge balance. It is expected that more mixed-metal borophosphates and borophosphate−phosphates with various types of open-framework structures and novel physical properties can be prepared by using similar synthetic methods in the near future.

Acknowledgment. This investigation was based on work supported by the National Natural Science Foundation of China under Project 20773131, the National Basic Research Program of China (Grant 2007CB815307), the Funds of Chinese Academy of Sciences (Grants KJCX2-YW-H01 and FJIRSM-SZD07001), and the Fujian Key Laboratory of Nanomaterials (Grant 2006L2005).

Supporting Information Available: X-ray crystallographic files in CIF format, atomic coordinates (Table S1), selected bond lengths (Table S2), simulated and experimental powder XRD patterns for compounds **1** and **2** (Figure S1), TGA and DTA diagrams for compounds **1** and **2** (Figure S2), UV absorption spectra (Figure S3) and IR spectra (Figure S4) for compounds **1** and **2**, and $M-H$ diagram for compound **2** (Figure S5). This material is available free of charge via the Internet at http://pubs.acs.org.